Interstrand Complex Formation of Purine Oligonucleotides and Their Nonionic Analogs: The Model System of d(AG) 8 and Its Complement, d(CT) 8 †

ARTICLE *in* BIOCHEMISTRY · MAY 1996

Impact Factor: 3.02 · DOI: 10.1021/bi960070b · Source: PubMed

5 AUTHORS, INCLUDING:

Richard I Hogrefe
TriLink BioTechnologies
27 PUBLICATIONS **808** CITATIONS

Interstrand Complex Formation of Purine Oligonucleotides and Their Nonionic Analogs: The Model System of $d(AG)_8$ and Its Complement, $d(CT)_8$[†]

Tina L. Trapane,[‡] Richard I. Hogrefe,[§] Mark A. Reynolds,[§,||] Lou-sing Kan,[‡,⊥] and Paul O. P. Ts'o*[,‡]

Department of Biochemistry, School of Hygiene and Public Health, The Johns Hopkins University, 615 North Wolfe Street, Baltimore, Maryland 21205, and Genta, Incorporated, 3550 General Atomics Court, San Diego, California 92121

Received January 11, 1996; Revised Manuscript Received March 5, 1996[⊗]

ABSTRACT: We have investigated the role of purines in interstrand complex formation with regard to substitution of the negatively-charged, phosphodiester backbone by a nonionic, internucleoside linkage. Using the purine oligomer, $d(AG)_8$, its methylphosphonate analog, $d(\underline{AG})_8$, and the complementary pyrimidine oligomer, $d(CT)_8$, as a model system, the stoichiometry, conformation, and stability of complexes formed at pH 8 were studied by spectroscopic and electrophoretic methods. When there is only one oligomer species in solution, $d(\underline{AG})_8$ behaves as a single-stranded molecule. In contrast, the $d(AG)_8$ oligomer readily forms an intermolecular self-complex, particularly in the presence of magnesium ion. Using either purine oligomer, duplexes can form with the $d(CT)_8$ strand which differ in terms of their conformation and in the dependence of their thermal stability on sodium and magnesium ions. All studies show that a stable triplex forms with a 1:2 $d(CT)_8$:$d(\underline{AG})_8$ stoichiometry which does not require high concentrations of sodium or magnesium ions. Triplex formation between the $d(CT)_8$ strand and two $d(AG)_8$ strands was not observed. Native gel electrophoresis suggests that a 1:1:1 $d(CT)_8$:$d(AG)_8$:$d(\underline{AG})_8$ complex may be formed. In regard to triplex formation, the advantage of the methylphosphonate backbone on the purine strand is clearly demonstrated.

Nucleic acid interactions which involve base-recognition motifs other than the familiar Watson−Crick (W·C)[1] T(U)·A and C·G base pairs have been the focus of many physical studies. In particular, interest in the formation of three-stranded helices, or triplexes, has been rekindled from two general aspects. (1) The ability of certain naturally-occurring sequences to adopt intramolecular triplex conformations (H-form) has led to the proposal that such structures may play roles *in vivo* (Wells et al., 1988). (2) Triplex formation through binding of a nucleotide probe to a double-stranded DNA target site has been proposed as a means of regulation of gene expression at the DNA level (Miller & Sobell, 1966; Cooney et al., 1988; Maher et al., 1989; François et al., 1989).

The most familiar triplex construct is one in which a pyrimidine third strand interacts with a pyrimidine·purine sequence in a W·C duplex (pyr·pur-pyr) (Felsenfeld et al., 1957; Lipsett, 1964; Morgan & Wells, 1968; Lee et al., 1979; Moser & Dervan, 1987; Rajagopal & Feigon, 1989). The third strand binds in a parallel orientation to the purine tract in the duplex via sequence-specific, Hoogsteen-type hydrogen bonds. Third-strand thymidine residues pair with adenines in T·A base pairs to form T·A-T base triads and protonated third-strand cytosine residues pair with guanosines in C·G base pairs to form $C\cdot G\text{-}C^+$ base triads. Therefore, formation of such triple-stranded complexes is dependent upon hydrogen ion concentration and occurs more readily at low pH.

A second triplex construct is one in which a purine-rich third strand binds to the purine tract of a W·C duplex (pyr·pur-pur). Triplexes of this type have been found to occur with homopolymer C·G-G (Lipsett, 1963; Marck & Thiele, 1978; Kohwi & Kohwi-Shigematsu, 1988), T(U)·A-A (Broitman et al., 1987; Howard et al., 1995), or C·G-A (Chastain & Tinoco, 1992) interactions. Most studies reported to date involve pyr·pur-pur triplex formation at mixed (C+T)·(G+A) W·C sites (Cooney et al., 1988; Bernués et al., 1990; Beal & Dervan, 1991; Pilch et al., 1991; Radhakrishnan et al., 1991; Malkov et al., 1993). In general, these studies show that the third strand binds in an antiparallel orientation to the underlying purine tract in the duplex. Guanosines in C·G base pairs hydrogen bond with guanosine residues in the third strand to form C·G-G base triads having a geometry found as a tertiary interaction in tRNA (Kim, 1987). Adenosine residues in T·A base pairs, however, can be recognized by either thymidine or adenosine residues in the third strand. The A-T second-third strand pairing has been shown to occur by reverse-Hoogsteen geometry (Radhakrishnan et al., 1991). The A-A pairing has been proposed to occur via a geometry also observed in tRNA (U·A-A tertiary interaction); however, the configuration of this pairing has yet to be verified by physical methods. Triplex formation utilizing purine-rich third strands in many cases requires a

[†] Supported by grants to P.O.P.T. from the National Cancer Institute (5 PO1 CA42762-05) and Department of Energy (DE-FG02-88ER60636). T.L.T. is a Genta, Inc., postdoctoral fellow.

* Corresponding author. Tel: (410) 955-3172. FAX: (410) 955-4392.

[‡] The Johns Hopkins University.

[§] Genta, Incorporated.

[||] Present address: Ribozyme Pharmaceuticals, Inc., Boulder, CO.

[⊥] Present address: Institute of Chemistry, Academia Sinica, Taipei, Taiwan.

[⊗] Abstract published in *Advance ACS Abstracts,* April 15, 1996.

[1] Abbreviations: CD, circular dichroism; C_T, total strand concentration; NMR, nuclear magnetic resonance; PAGE, polyacrylamide gel electrophoresis; pyr·pur, pyrimidine·purine duplex; pyr·pur-pur, pyrimidine·purine-purine triplex; pyr·pur-pyr, pyrimidine·purine-pyrimidine triplex; T_m, temperature at helix−coil transition midpoint; UV, ultraviolet; W·C, Watson−Crick.

S0006-2960(96)00070-0 CCC: $12.00

high proportion of guanosine residues arranged in clusters at the double-stranded target site and the presence of specific cations.

Nonionic nucleic acid analogs having methylphosphonate, internucleoside backbone linkages (O3′-POCH$_3$-O5′) have been a subject of interest in this laboratory. These molecules are resistant to enzymatic digestion and may be taken up by cells in culture (Miller et al., 1980, 1981; Shoji et al., 1991; Thaden & Miller, 1993). Thus, they can serve as model compounds to probe or to modulate the function of nucleic acids within living systems. The absence of electrostatic repulsive forces at the nonionic backbone of these analogs should favor complex formation with negatively-charged nucleic acid target sequences. However, particular stereoconfigurations of the methyl group at the chiral phosphonate linkage may adversely effect complex formation through steric interactions (Miller et al., 1980; Bower et al., 1987; Lesnikowski et al., 1990). We have previously reported the formation of hybrid phosphodiester−methylphosphonate pyr·pur-pyr triplexes (Miller et al., 1980, 1981; Callahan et al., 1991). However, it has been reported that similar complexes do not form in a model system of dT (or dU) and dA oligomers (Kibler-Herzog et al., 1990).

In the studies reported here, we compare the purine oligomer, d(AG)$_8$, and its nonionic methylphosphonate analog, d(<u>AG</u>)$_8$, in their ability to form either a pyr·pur duplex or a pyr·pur-pur triplex with the complementary pyrimidine oligomer, d(CT)$_8$, as well as their self-association behavior. Ultraviolet (UV), circular dichroism (CD), and nuclear magnetic resonance (NMR) spectroscopies were utilized to examine the stoichiometry, structure, and thermal stability of interstrand complexes which form. The effects of sodium and magnesium ions on complex formation were also addressed. In addition, native polyacrylamide gel electrophoresis (PAGE) was used to physically separate and visualize the types of complexes which can form. In regard to triplex formation, the advantage of the methylphosphonate backbone on the purine strand is clearly demonstrated. In an earlier investigation, the d(<u>AG</u>)$_8$ oligomer was investigated in regard to complex formation with its RNA complement, (CU)$_8$. Physical and biochemical methods were employed to demonstrate that a stable 1:2 (CU)$_8$:d(<u>AG</u>)$_8$ triplex is formed which can arrest protein translation and reverse transcription activity *in vitro* (Reynolds et al., 1994).

EXPERIMENTAL PROCEDURES

Synthesis, Purification, and Characterization of Oligomers. The phosphodiester oligomers, d(AG)$_8$ and d(CT)$_8$, were synthesized on an Applied Biosystems 380A automated DNA synthesizer using standard cyanoethyl phosphoramidite methods. The methylphosphonate oligomer, d(<u>AG</u>)$_8$, was synthesized on a MilliGen/Biosearch 8750 automated synthesizer using methylphosphonamidite chemistry (Miller et al., 1991). Synthesis was terminated by the coupling of an adenine phosphoramidite monomer, resulting in one phosphodiester at the 5′-internucleoside linkage. This charged linkage facilitates purification and solubilization of the otherwise nonionic oligomer and also renders it a substrate for enzymes. Oligomers were purified by preparative HPLC and characterized by analytical HPLC, proton NMR, and ^{32}P end-labeling followed by denaturing PAGE. Extinction coefficients, ϵ_{254} ($mM^{-1}\cdot cm^{-1}$), for d(AG)$_8$ of 147 and d(CT)$_8$ of 98 in 0.01 M sodium phosphate, 0.01 mM EDTA, pH 7, were determined by snake venom phosphodiesterase I digestion (Trapane, 1993). The d(<u>AG</u>)$_8$ methylphosphonate oligomer was digested with piperidine (Callahan et al., 1991) to give an ϵ_{254} of 193 in the same buffer having 25% CH_3CN/H_2O (v/v) as solvent.

Sample Preparation and Conditions. An initial mixing study at pH 7 in 0.1 M NaCl showed the formation of a pyr·pur-pyr triplex at 2:1 d(CT)$_8$:d(<u>AG</u>)$_8$ molar ratio. The pH dependence of CD spectra for the 2:1 mixture at 20 °C gives an apparent pK_a of 7 for d(CT)$_8$·d(<u>AG</u>)$_8$-d(C$^+$T)$_8$ triplex formation (Lee et al., 1979; Callahan et al., 1991; Trapane, 1993). In order to avoid formation of this complex in the studies reported here, all experiments were performed at pH 8. Total concentration of all oligomer species in the sample, C_T, is given per strand. Samples were prepared by drying aliquots of stock solutions of the desired oligomers, dissolving in buffer, heating to 70 °C for 5 min, cooling slowly to room temperature, and equilibrating at 4 °C overnight. In general, the same samples were used for both CD and UV experiments. Studies with sodium counterion were performed in 0.01 M sodium phosphate, 0.01 mM EDTA, pH 8. Sodium ion concentration was increased by addition of the dry chloride salt, and the activity of the cation was calculated for NaCl according to a Guggenheim function (Harned & Owen, 1967). Samples to which magnesium ion was added were prepared in 0.1 M NaCl, 0.01 M Tris-HCl, pH 8. Magnesium ion concentration was increased by the addition of microliter aliquots of concentrated $MgCl_2$. The effect of sample dilution was taken into account when reporting the value of $\Delta\epsilon$ in the CD studies.

UV Mixing Curves. Continuous variation titrations (Job, 1928) were performed with pairs of samples beginning with 2.4 μM of either pyrimidine or purine oligomer. The titration involving the parent duplex and the nonionic purine strand began with one sample having 2.4 μM each of the complementary phosphodiester oligomers and the other with 2.4 μM of the methylphosphonate oligomer. UV absorbance was monitored at room temperature (22−24 °C) on a Varian DMS-100 spectrophotometer in 1 cm pathlength cells. Exchanges at 5% mole fraction intervals were made using paired, variable-volume pipettes. The solutions were mixed with stirring bars placed in the cuvettes and allowed to equilibrate at least 2 h at room temperature between each titration point.

CD Spectroscopy. CD spectra were obtained on an AVIV 60DS spectropolarimeter using a 1 cm quartz fluorescence cuvette containing 1.5 mL samples at 4.8 μM C_T. Temperature was maintained at 20 °C by fluid circulating through the cuvette holder from a cooling bath. Spectra were recorded at 1 nm increments from 350 to 205 nm with a constant bandwidth of 0.8 nm and are the average of three scans. The instrument was calibrated using (1*S*)-(+)-10-camphorsulfonic acid (Johnson, 1985), and $\Delta\epsilon$ ($M^{-1}\cdot cm^{-1}$) is reported per residue. Base line correction, scaling, data smoothing, and spectral calculations were performed using the AVIV plot program. A third-order polynomial averaged over a 7 nm bandwidth was used to smooth the observed spectra.

UV Thermal Profiles. Absorption *vs* temperature profiles were obtained on a Varian 219 spectrophotometer monitored at the absorption maximum for the pyr:pur complexes and at 255 nm for the purine strands alone. Standard C_T was

4.8 μM. Sample heating and cooling rates of 0.5 °C per minute were controlled by fluid circulating from a programmable temperature bath. The midpoint temperature (T_m) for a cooperative helix−coil transition is defined as the temperature at one-half of the absorbance change after correction for pre- and post-transitional base lines. Apparent T_m's for the broad transitions observed for self-association of the $d(AG)_8$ oligomer were determined from the maximum of d*A*/d*T* *vs* temperature curves. All profiles were thermally reversible, giving T_m values within one degree for both heating and cooling cycles.

Thermodynamics of helix−coil transitions for the complexes in 0.1 M sodium ion were obtained from shape analysis of the thermal profiles (Albergo et al., 1981). Briefly, the two-state equilibrium for association of a duplex in the model system is

$$d(CT)_8 + d(AG)_8 \rightleftharpoons d(CT)_8 \cdot d(AG)_8 \quad (1)$$

For 1:1 mixtures of strands which are not self-complementary, the equilibrium constant for association, K_{assoc}, may be expressed in terms of the fraction of strands in the duplex, α, and of the total strand concentration, C_T, as

$$K_{assoc} = \frac{[d(CT)_8 \cdot d(AG)_8]}{[d(CT)_8][d(AG)_8]} = \frac{\alpha}{2(1-\alpha)^2 C_T} \quad (2)$$

After subtraction of pre- and post-transitional base lines, the observed cooperative profile is used to calculate the fraction of strands in double- and single-stranded states and to derive the equilibrium constant at each temperature throughout the transition. The midpoint of the helix−coil transition in this type of analysis is defined as the temperature at which the fraction of strands in duplex form is equivalent to the fraction in single-stranded form ($\alpha = 1 - \alpha$). A plot of the calculated K_{assoc} as a function of inverse absolute temperature should be best fit by a straight line for a two-state, single-transition model. Thermodynamics of complex formation can be derived from the slope and intercept of this line according to the relationship of van't Hoff where

$$\ln K_{assoc} = -\frac{\Delta H^\circ}{R} T^{-1} + \frac{\Delta S^\circ}{R} \quad (3)$$

The profile of the 1:2 $d(CT)_8$:$d(\underline{AG})_8$ mixture was analyzed by two different equilibrium models:

$$d(CT)_8 + d(\underline{AG})_8 + d(\underline{AG})_8 \rightleftharpoons d(CT)_8 \cdot d(\underline{AG})_8\text{-}d(\underline{AG})_8 \quad (4)$$

(single-strands to triplex); and

$$d(CT)_8 + d(\underline{AG})_8 + d(\underline{AG})_8 \rightleftharpoons d(CT)_8 \cdot d(\underline{AG})_8 + d(\underline{AG})_8 \quad (5)$$

(single-strands to duplex with noninteracting equivalent of purine strand). Expressions for association binding constants for these two models may be written as:

$$K_{assoc} = \frac{[d(CT)_8 \cdot d(\underline{AG})_8\text{-}d(\underline{AG})_8]}{[d(CT)_8][d(\underline{AG})_8]^2} = \frac{9\alpha}{4(1-\alpha)^3 C_T{}^2} \quad (6)$$

and

$$K_{assoc} = \frac{[d(CT)_8 \cdot d(\underline{AG})_8]}{[d(CT)_8][d(\underline{AG})_8]} = \frac{3\alpha}{2(1-\alpha)^2 C_T} \quad (7)$$

respectively. All other considerations remain as for analyses of duplex transitions.

NMR Spectroscopy. Hydrogen-bonded imino proton resonances were observed on a Bruker WM-300 NMR spectrometer in 0.1 M sodium(chloride), 0.01 M (sodium)-phosphate, 0.1 mM EDTA, pH 8, having 9:1 ^1H_2O:^2H_2O as solvent. A $1\bar{3}3\bar{1}$ pulse sequence was used for solvent suppression (Hore, 1983) with maximum excitation centered in the imino proton region. Chemical shifts are reported with respect to external sodium 2,2-dimethyl-2-silapentane-5-sulfonate at 0 ppm and are temperature corrected. Probe temperature was maintained by a BVT-1000 regulator. The $d(CT)_8$:$d(\underline{AG})_8$ [1 mM]:[1 mM] sample was prepared in a microcentrifuge tube in 0.4 mL of buffer and transferred to a 5 mm tube. After NMR spectra of the hybrid duplex were obtained, this sample was transferred into another microcentrifuge tube containing an additional equivalent of $d(\underline{AG})_8$, lyophilized, dissolved in 0.4 mL of solvent, and returned to the NMR tube for observation of the hybrid triplex. The samples at both stoichiometries of pyr:pur strand dissolved readily, resulting in clear, colorless solutions.

Gel Electrophoresis. Oligomers were labeled at the 5′-end with [γ-^{32}P]ATP using T4 polynucleotide kinase. Sample preparation and running buffer was 0.1 M NaCl, 0.04 M Tris, 0.01 M H_3PO_4, 1 mM EDTA, pH 8. Labeled oligomers along with unlabeled, unphosphorylated oligomers were dried at the indicated concentrations and stoichiometric ratios, dissolved in 10 μL of buffer, and annealed as for the optical samples. The $d(CT)_8$:$d(AG)_8$:$d(\underline{AG})_8$ samples were prepared by annealing parent duplexes to 4 °C, transferring the solutions to tubes on ice containing dried $d(\underline{AG})_8$, and equilibrating at 4 °C for 3 h before loading on the gel. Ficoll-400 loading buffer (2 μL, 15%) was added immediately prior to loading a 6 μL volume of each sample on a 40 × 31 × 0.04 cm 16% polyacrylamide gel (19:1 acrylamide:bisacrylamide). Electrophoresis was carried out at 4 °C, 2.5 V/cm (12 mA), for 36 h with buffer recirculation to prevent pH changes. The gel was dried and autoradiographed for 3 h at −80 °C.

RESULTS

UV Mixing Curves. The stoichiometry of interstrand complexes formed between complementary oligomers in the model system can be determined by monitoring the absorption of solutions having continuously varying proportions of the interacting strands (Job, 1928; Felsenfeld et al., 1957). The principle of these type of experiments is that absorbance breakpoints should be observed at the exact molar ratio of interacting strands in a specific complex. Breakpoints are usually hypochromic, resulting from differential base-stacking interactions in complexed and uncomplexed states. A mixing curve for the phosphodiester oligomers at room temperature in 0.1 M sodium ion (Figure 1A) yields a single endpoint at 0.5:0.5 $d(CT)_8$:$d(AG)_8$ molar ratio, indicating formation of the expected W·C parent duplex. When $d(CT)_8$ is titrated with the nonionic $d(\underline{AG})_8$ oligomer at the same condition, however, two breakpoints are observed. Shown in Figure 1B is the dependence of the absorbance at 270 nm on molar ratio of pyr:pur strand. The endpoint at 0.5 mole

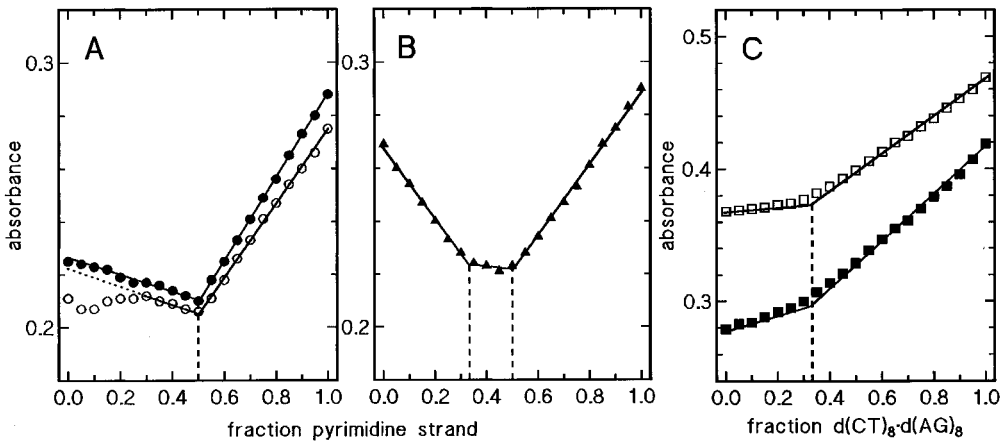

FIGURE 1: Continuous variation titrations. Stoichiometry of pyr:pur interactions at room temperature, pH 8. (A) $d(CT)_8$:$d(AG)_8$ at 270 nm in 0.1 M Na^+ [●] and 0.1 M Na^+, 0.05 M Mg^{2+} [○]. (B) $d(CT)_8$:$d(\underline{AG})_8$ at 270 nm in 0.1 M Na^+ [▲]. (C) $d(CT)_8$·$d(AG)_8$:$d(\underline{AG})_8$ at 270 [■] and 250 [□] nm in 0.1 M Na^+. UV absorbance is plotted as a fraction of pyrimidine strand in A and B or as a fraction of $d(CT)_8$·$d(AG)_8$ duplex in C.

fraction $d(CT)_8$ indicates formation of a W·C-type duplex, hereafter referred to as the hybrid duplex. An additional endpoint at 0.33:0.67 $d(CT)_8$:$d(\underline{AG})_8$ is evidence for formation of a complex having 1:2 pyr:pur strand stoichiometry (hybrid triplex). Also shown in Figure 1A is a mixing curve for the phosphodiester oligomers with additional 0.05 M magnesium ion. Although there are some deviations from linearity at greater than 0.7 mole fraction purine strand, only one clear endpoint at duplex stoichiometry is observed. The nonlinear change in absorbance at high purine strand ratios may be due to disruption of a self-associated $d(AG)_8$ complex upon formation of the pyr·pur duplex. In support of this argument, the UV spectrum of $d(AG)_8$ by itself has decreased intensity compared to that observed for the $d(\underline{AG})_8$ analog, especially in the presence of divalent cation. This relative hypochromism for the phosphodiester purine oligomer indicates that its secondary structure is substantially greater than that of the methylphosphonate analog. Comparisons at a single wavelength can give only qualitative information regarding base stacking and secondary structure; however, it should be noted that formation of the hybrid triplex and duplex results in approximately the same amount of hypochromicity at 270 nm as for the parent duplex in 0.1 M sodium ion. Note that endpoints at 2:1 pyr:pur stoichiometry are not observed, indicating that pyr·pur-pyr triplexes do not form in this system at pH 8.

The continuous variation method was also used to investigate the possibility of the nonionic $d(\underline{AG})_8$ oligomer binding as a third strand to the parent duplex, $d(CT)_8$·$d(AG)_8$, having both strands with phosphodiester backbone. Such a system would be the model for a methylphosphonate purine oligomer binding to a pyr·pur target site within double-stranded DNA, resulting in the formation of a pyr·pur-pur triplex. However, the possibility of displacement of the original $d(AG)_8$ strand in the parent duplex for the added $d(\underline{AG})_8$ strand will be of concern in a model system using oligomers of equivalent length. A solution of $d(\underline{AG})_8$ at 2.4 μM strand concentration was mixed with a solution containing 2.4 μM each of $d(CT)_8$ and $d(AG)_8$. Absorbances at two wavelengths are shown in Figure 1C, where only a single, broad endpoint is observed at 1:2 molar ratio of duplex: $d(\underline{AG})_8$. The stoichiometry of this endpoint indicates that strand displacement is indeed taking place. The equilibrium in such a system can be expressed as follows:

$$d(CT)_8{\cdot}d(AG)_8 + 2[d(\underline{AG})_8] \rightleftharpoons d(CT)_8{\cdot}d(\underline{AG})_8\text{-}d(\underline{AG})_8 + d(AG)_8$$

This result indicates that the model system utilizing oligomers of equal length may not be useful to investigate the formation of a pyr·pur-pur intermolecular triplex. However, it is interesting to note that the nonionic purine strand can displace its negatively-charged counterpart as a complement for $d(CT)_8$, indicating that formation of the hybrid triplex is more favorable than formation of the parent duplex at these conditions.

CD Spectroscopy. Conformations of the oligomers as single strands or within intermolecular complexes may be analyzed by comparison of circular dichroic properties of the base chromophores. CD spectra at 20 °C of the individual oligomers and their stoichiometric mixtures are given in Figure 2. Both phosphodiester (panel A) and methylphosphonate (panel B) purine strands in 0.1 M sodium ion have similar spectra characterized primarily by a negative band near 287 nm and a strong positive band near 212 nm. The most notable differences between these "single-strand" spectra are observed in the positive bands at intermediate wavelength (280−240 nm). The spectrum of the phosphodiester pyrimidine oligomer, $d(CT)_8$ (panel B), is similar to that found for single-stranded poly[d(CT)] at neutral pH (Gray et al., 1987). CD spectra of mixtures at 1:1 molar ratio of pyr:pur strand in 0.1 M Na^+ are shown in panels A and B for the parent and hybrid duplexes, respectively. The observed spectra of each mixture is quite different from additive spectral contributions of the individual free strands, indicating formation of a specific complex in each case. Changes in base-stacking interactions upon going from single-stranded oligomers to double-stranded helical structures are responsible for these unique CD patterns. However, the two complexes show marked differences in the 300−240 nm range. The spectrum of the parent duplex (panel A) is almost identical in shape and magnitude to that reported for poly[d(CT)·d(AG)] at pH 8.4 in 10 mM sodium phosphate (Gray et al., 1987) and is typical of a B-form helix, with positive and negative bands at 278 and 241 nm, respectively. In comparison, the CD spectrum of the hybrid duplex (panel B) is unusual in that there are additional negative bands at 295 and 263 nm and the positive band near 280 nm is reduced in magnitude. Absence of negative

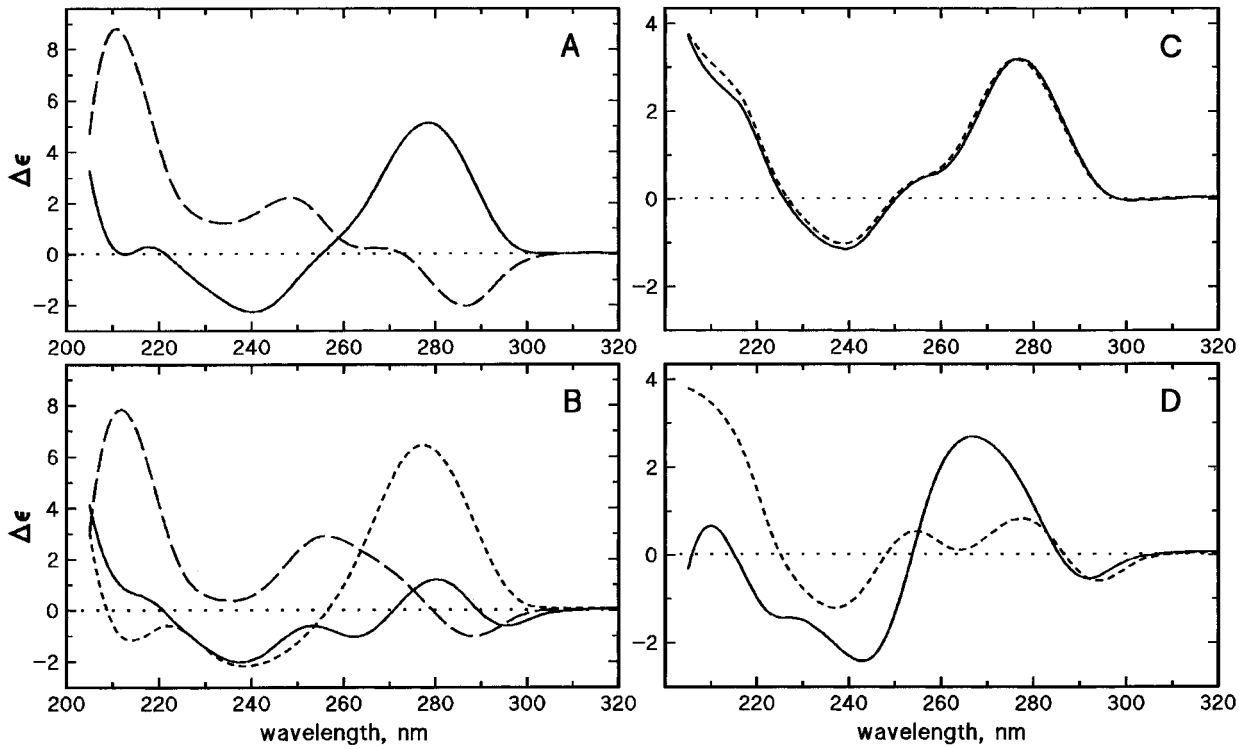

FIGURE 2: CD spectra observed and calculated for oligomers and their stoichiometric mixtures at pH 8 in 0.1 M Na^+, 20 °C. (A) $d(AG)_8$ phosphodiester oligomer [− −] and $d(CT)_8$:$d(AG)_8$ 1:1 mixture (parent duplex) [—]. (B) $d(\underline{AG})_8$ methylphosphonate oligomer [− −], $d(CT)_8$ phosphodiester oligomer [- - -] and $d(CT)_8$:$d(\underline{AG})_8$ 1:1 mixture (hybrid duplex) [—]. (C) Observed spectrum for 1:2 $d(CT)_8$:$d(AG)_8$ mixture [—] and weighted sum of spectra for the parent duplex and $d(AG)_8$ oligomer (1:1) [- - -]. (D) Observed spectrum for 1:2 $d(CT)_8$:$d(\underline{AG})_8$ mixture [—] and weighted sum of spectra for the hybrid duplex and $d(\underline{AG})_8$ oligomer (1:1) [- - -].

charge and the presence of methyl groups in the methylphosphonate backbone should not change intrinsic base absorption properties. Moreover, the chiral methylphosphonate linkages do not contribute to the absorption spectrum in this region. Therefore, comparison of CD spectra indicates that the conformations of parent and hybrid duplexes are not equivalent.

CD spectra observed for 1:2 mixtures of pyr:pur strands, along with spectra calculated for such mixtures are shown in Figure 2, panels C and D. One equivalent of purine strands in such mixtures will form a duplex with the $d(CT)_8$ strand. If the additional equivalent of purine strand does not interact with this duplex to form a new complex, then it should be possible to reproduce the observed CD spectrum by taking the weighted sum of spectra observed for the duplex and a "free" purine strand. As shown in panel C, this is the case for the $d(CT)_8$:$d(AG)_8$ 1:2 mixture in 0.1 M sodium ion, indicating that a complex of higher purine strand stoichiometry does not form with the phosphodiester purine oligomer. The observed spectrum is nearly identical to a spectrum calculated for the parent duplex and a noninteracting $d(AG)_8$ strand. On the other hand, the $d(CT)_8$:$d(\underline{AG})_8$ 1:2 mixture cannot be approximated by such analysis (panel D), consistent with formation of a new complex, the hybrid triplex. The spectrum observed for this complex is unique, most notably in that the positive band has shifted from 281 nm for the hybrid duplex to 266 nm for the hybrid triplex. Also, there are changes in position and magnitude of bands near 290, 240, and 210 nm. The CD spectrum observed for this triplex comprised of three deoxyribose backbone oligomers is very similar to that observed for the hybrid triplex formed by an RNA pyrimidine strand, $(CU)_8$, and two $d(\underline{AG})_8$ strands (Reynolds et al., 1994).

Effects of magnesium ion on the structure of the oligomers and their intermolecular complexes are readily assayed by changes in their CD spectra observed upon addition of the divalent cation (Figure 3). Titration of the phosphodiester purine oligomer, $d(AG)_8$, with $MgCl_2$ at 20 °C results in dramatic changes in the CD. Several spectra obtained during this titration are overlaid in panel A where an isoelliptic point at 252 nm and an increase in the magnitude of the bands at 263 and 244 nm are clearly seen. Mg^{2+}-dependent ellipticity changes at these two wavelengths (panel B) show that effects on the structure of the negatively-charged purine oligomer are not complete until approximately 0.3 M. The resulting spectrum at high magnesium ion concentration for $d(AG)_8$ is comparable to spectra reported for the same purine dinucleotide sequence at various conditions by others (Lee et al., 1979; Antao et al., 1988; Rippe et al., 1992; Dolinnaya & Fresco, 1992). Such spectral changes for the negatively-charged $d(AG)_8$ oligomer, in the absence of its complementary strand, indicate an increase in self-structure. The titration isoelliptic point is coincident with the absorption maximum of guanosine and the positive and negative bands which develop at 263 and 244 nm are centered around this point at equivalent frequency differences. These spectral characteristics are consistent with coupled exiton interactions of guanosine $\pi-\pi^*$ transitions (Bush, 1974), suggesting that these residues are directly involved in the structural change induced by the divalent cation. Addition of magnesium ion to the $d(CT)_8$ or $d(\underline{AG})_8$ oligomers results in the same CD spectra as those observed in 0.1 M sodium ion (data not shown); therefore, the divalent cation has no apparent effect on the structure of these oligomers as single strands.

The phosphodiester purine oligomer was unable to form a triplex with the parent duplex in 0.1 M sodium ion, as

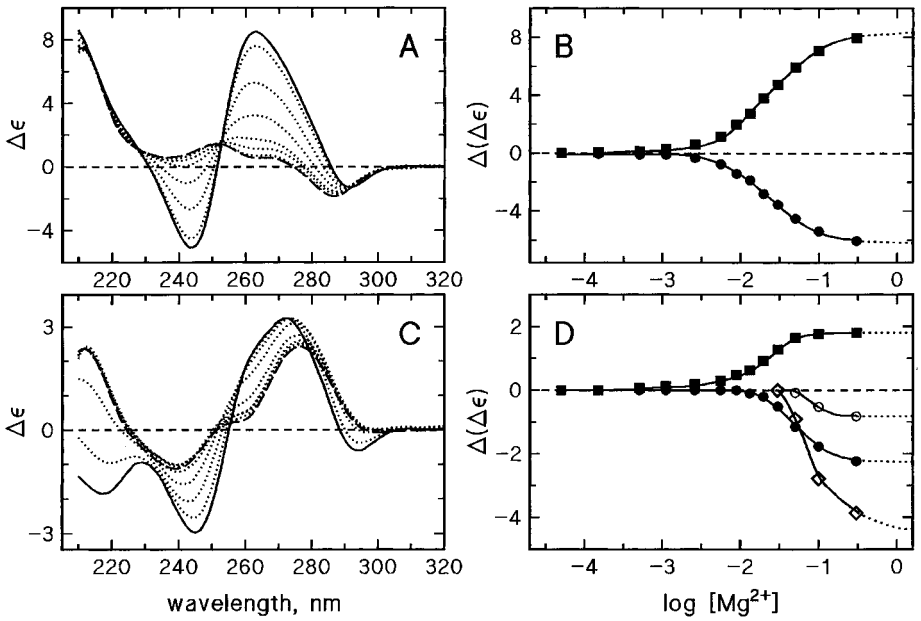

FIGURE 3: Magnesium ion effects on interstrand interactions of the purine phosphodiester oligomer, $d(AG)_8$, at pH 8 in 0.1 M Na^+, 20 °C. (A) Overlay of CD spectra for $d(AG)_8$ oligomer without additional $MgCl_2$ [− −], with increasing concentrations of $MgCl_2$ [···] and with 0.3 M $MgCl_2$ [—]. (B) Mg^{2+} induced CD spectral changes for $d(AG)_8$ at 263 [■] and 244 [●] nm. (C) Overlay of CD spectra for $d(CT)_8$:$d(AG)_8$ 1:2 mixture (representation as in panel A). (D) Mg^{2+} induced CD spectral changes for the $d(CT)_8$:$d(AG)_8$ 1:2 mixture at 290 [○], 260 [■], 246 [●], and 213 [◇] nm. In B and D, $\Delta(\Delta\epsilon)$ is the difference between a reference spectrum in the absence of ion ($\Delta\epsilon_{0Mg}$) and spectra with added Mg^{2+} ($\Delta\epsilon_{+Mg}$).

demonstrated by UV mixing curves and CD spectral calculations above. In the event that magnesium ion could induce binding of $d(AG)_8$ as a third strand, CD spectra of a 1:2 $d(CT)_8$:$d(AG)_8$ mixture were observed as a function of $MgCl_2$ concentration and ellipticity changes were monitored (Figure 3, panels C and D). The major features of the 1:2 mixture of pyr:pur oligomers reflect the parent duplex up to ~1 mM ion. Isoelliptic points are not observed at low cation concentrations. At higher Mg^{2+} concentrations (2−30 mM), positive and negative bands near 260 and 245 nm begin to increase in magnitude and an isoelliptic point appears near 252 nm. These features are at similar wavelengths and show a similar dependence on divalent ion activity as for the $d(AG)_8$ oligomer by itself. Such spectral changes may be attributed to the self-association of the excess equivalent of purine strand not involved in formation of the duplex. Above 0.05 M Mg^{2+}, negative bands at 290 and 213 nm begin to develop and isoelliptic points shift to increasingly longer wavelengths. These results indicate that the excess purine strand is interacting with the duplex, either singly or as its self-complex. However, the CD spectral changes are incomplete up to the highest concentration of Mg^{2+} attained in the titration (0.3 M). Requirement of such an excess of divalent cation to induce the structural alterations reflected in the CD spectra of the 1:2 pyr:pur mixture, makes its relevance to a possible physiological complex quite remote. The CD spectra of both parent and hybrid duplexes as well as the hybrid triplex are not affected by the addition of up to 0.05 M $MgCl_2$ (data not shown). These results indicate that magnesium ion has an effect on the ability of the phosphodiester purine oligomer to associate with itself in the formation of a self-complex, and, at high concentrations, may enable some interaction of this self-complex with the parent duplex. The divalent cation does not appear to affect the conformations of the other oligomers or intermolecular complexes formed in the model system. Although the relative intensities of their spectra are quite different, note that the $d(AG)_8$ self-complex (Figure 3A) and the hybrid triplex (Figure 2D) have some features in common above 240 nm, namely, negative bands at 290 and 243 nm and a positive band near 265 nm.

UV Thermal Profiles. Thermal stabilities and characteristics of helix−coil transitions for the various complexes can be determined from the temperature dependence of their UV spectra. Absorbance *vs* temperature profiles for stoichiometric mixtures of $d(CT)_8$ with $d(AG)_8$ or $d(\underline{AG})_8$ in 0.1 M sodium ion are shown in Figure 4A. Cooperative, monophasic transitions are observed for the parent duplex as well as for the hybrid duplex and triplex. These helix−coil transitions are sharp and well-defined and, except for the hybrid duplex, show little pre-transition hyperchromicity. The increased base line above 20 °C observed in the profile of the 1:1 $d(CT)_8$:$d(\underline{AG})_8$ mixture may be due to an effect of diastereoisomer heterogeneity of the methylphosphonate oligomer on the thermal stability of the complex or to some population of the hybrid triplex state in the 1:1 mixture. At this ionic strength all of the complexes have T_m's of approximately 50 °C. The thermal behavior of the hybrid triplex and parent duplex suggests that formation of these complexes may be approximated by a two-state, all-or-none process. While this observation is not unexpected for W•C duplexes, it is not necessarily the case to be expected for the hybrid triplex. Thermal studies on triplexes formed by the intermolecular interactions of oligomers generally exhibit biphasic transitions in which the third strand dissociates from the underlying W•C duplex at temperatures well below the duplex helix−coil transition (Broitman et al., 1987; Pilch et al., 1990; Plum et al., 1990). The interpretation for such systems is that energetics for binding of the third strand to the duplex are less favorable than for formation of the duplex itself. However, in the hybrid triplex studied here, the thermal profile indicates that the system goes directly from

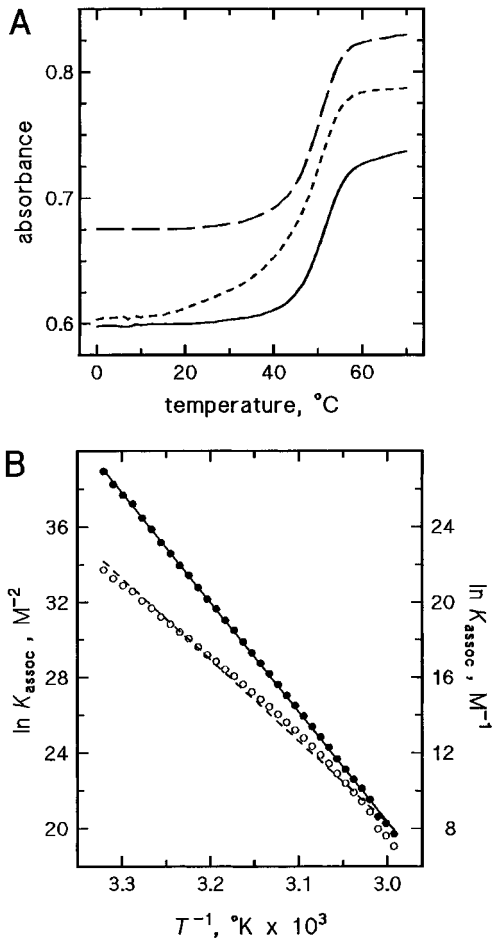

FIGURE 4: Temperature dependence of UV absorbance for the parent duplex and the hybrid duplex and triplex at pH 8 in 0.1 M Na^+. (A) $d(CT)_8$:$d(AG)_8$ 1:1 at 258 nm [—], $d(CT)_8$:$d(\underline{AG})_8$ 1:1 at 259 nm [- - -], and $d(CT)_8$:$d(\underline{AG})_8$ 1:2 at 259 nm [— —]. (B) Van't Hoff plots for the thermal profile of the $d(CT)_8$:$d(\underline{AG})_8$ 1:2 mixture analyzed according to eq 4 (●, left ordinate) or eq 5 (○, right ordinate) association models.

a three-stranded complex to single strands. An intermediate duplex state is not observed. Although the structure and, therefore, the energetics of the underlying hybrid duplex are expected to change upon binding of the second purine strand, this observation suggests that interactions of the third strand with the duplex are at least as favorable as W·C interactions in the duplex.

The standard state changes in enthalpy and entropy for the formation of the intermolecular complexes formed at 0.1 M sodium ion were obtained by shape analysis of their thermal profiles (Table 1). The model-derived values of $\Delta H°$ and $\Delta S°$ per base residue for the parent duplex are within accepted values for oligomers having the same nearest-neighbor sequence composition (Breslauer et al., 1986). The hybrid duplex shows less enthalpy gained on complex formation which is balanced by a decrease in the entropy penalty on going from the single-stranded to the more structured helical state. The thermal profile of the 1:2 $d(CT)_8$:$d(\underline{AG})_8$ mixture may be analyzed by two different equilibrium models in order to see which best describes the association behavior of the system (see Experimental Procedures). If the reaction were three strands associating to form a triplex, then the equilibrium is expressed as in eq 4. If only two complementary strands interact in the mixture to form a duplex with the excess equivalent of purine strand free in solution, then the equilibrium should be expressed as in eq 5. As only one transition is observed, a three-state (single-strands ⇌ duplex + third strand ⇌ triplex), two-transition equilibrium cannot be considered here. Calculated curves for the inverse temperature dependence of K_{assoc} for these two equilibria are shown in Figure 4B. The model for association of a triplex is described quite well by a straight line, whereas that for association of a duplex plus a non-interacting $d(\underline{AG})_8$ strand shows systematic deviation from linearity. Therefore, the shape of the thermal profile for the 1:2 $d(CT)_8$:$d(\underline{AG})_8$ mixture is consistent with a two-state, coil-to-triplex association. The calculated equilibrium binding constant is dependent on a C_T^2 term; therefore, values of $\Delta H°$ and $\Delta S°$ are larger for association of three strands in the formation of a triplex than for association of two strands in the formation of a duplex. It is interesting to note that the calculated free energy of formation near room temperature, $\Delta G°$(298 K), is nearly 40 kJ·mol^{-1} more favorable for the hybrid triplex than for the parent duplex. Conversion of these standard free energies into binding constants at room temperature results in K_{assoc} of 9×10^{12} M^{-1} for the parent duplex and 5×10^{19} M^{-2} for the hybrid triplex. These estimations of the relative stabilities of the two complexes are consistent with the endpoint observed in the mixing curve obtained for interaction of $d(\underline{AG})_8$ with the $d(CT)_8$·$d(AG)_8$ duplex (Figure 1C). The 1:2 duplex: $d(\underline{AG})_8$ endpoint results from displacement of the phosphodiester purine strand as a complement for the $d(CT)_8$ strand in order to form the more stable $d(CT)_8$·$d(\underline{AG})_8$-$d(\underline{AG})_8$ triplex.

Dependence of thermal stabilities on sodium ion activity for the parent duplex and the hybrid complexes are shown in Figure 5. As expected for interactions between negatively-charged strands, transition midpoints of the parent duplex are quite dependent upon monovalent cation activity, increasing by 26° over 1.5 orders of magnitude of ionic strength. In contrast, the two hybrid complexes show very little change in stability over the same range. The T_m of the hybrid duplex increases slightly before decreasing above 0.1 ion activity with an overall range of approximately 3°. The hybrid triplex is slightly more stable than the hybrid duplex at all sodium ion activities and exhibits only a monotonic decrease in stability of 2° over the range. Decreased T_m for the hybrid complexes as well as deviation from linearity for the parent duplex observed at high sodium ion activity may

Table 1: Thermodynamic Parameters of Helix−Coil Transitions in 0.1 M NaCl at pH 8[a]

oligomers	mole ratio	T_m (°C)	$\Delta H°$ [b] (kJ mol^{-1})	$\Delta S°$ [b] (J K^{-1} mol^{-1})	$\Delta G°$(298 K)[b] (kJ mol^{-1})
$d(CT)_8$:$d(AG)_8$	1:1	50.5	−506 [−31.6]	−1449 [−90.6]	−73.9 [−4.62]
$d(CT)_8$:$d(\underline{AG})_8$	1:1	50	−426 [−26.6]	−1208 [−75.5]	−66.0 [−4.13]
$d(CT)_8$:$d(\underline{AG})_8$	1:2	50	−601 [−37.6]	−1638 [−102.4]	−112.4 [−7.03]

[a] From shape analysis of UV thermal profiles. [b] Values in brackets are given per mole of base residue [16 residues/strand].

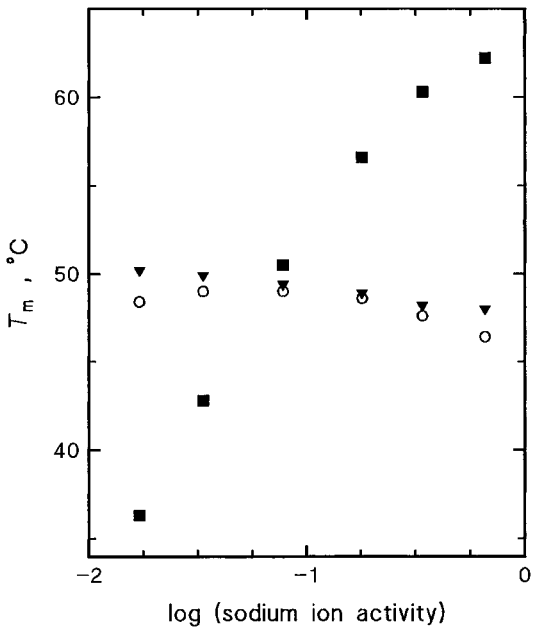

FIGURE 5: Dependence of T_m on sodium ion activity for interstrand pyr:pur complexes at pH 8. d(CT)$_8$:d(AG)$_8$ 1:1 [■], d(CT)$_8$:d(AG)$_8$ 1:1 [○], d(CT)$_8$:d(AG)$_8$ 1:2 [▼].

be due to ionic-strength-dependent differences in hydration of these complexes (Record et al., 1978). Magnesium ion effects on thermal profiles for the stoichiometric pyr:pur complexes formed in the model system were also explored. Addition of 0.05 M $MgCl_2$ to the hybrid duplex and triplex in 0.1 M sodium ion does not affect either the shape or the position of their helix−coil transitions. A seven degree increase in the T_m of the parent duplex results upon addition of 0.05 M $MgCl_2$. This is well within the expected range for divalent cation stabilization of helix−coil transitions observed for nucleic acid duplexes (Record et al., 1978).

Interstrand interactions of the individual oligomers in the model system were also investigated by the temperature dependence of their UV spectra. Thermal profiles for the two purine oligomers are shown in Figure 6A. The absorbance of the nonionic d(AG)$_8$ oligomer has a hyperchromicity of 9% from 0 to 70 °C, which is almost identical for samples in both 0.1 M sodium ion as well as with additional 0.05 M magnesium ion. The negatively-charged d(AG)$_8$ oligomer, on the other hand, has a profile in 0.1 M NaCl that has marked decreased absorbance at low temperatures with an overall hyperchromicity of 22%. Addition of 0.05 M $MgCl_2$ results in a profile exhibiting cooperative thermal behavior, with an apparent T_m more than 10° higher than the profile observed in sodium ion only. However, the breadth of this transition and the pre- and post-transitional absorbance slopes are notably greater than those observed for the stoichiometric complexes which form with the complementary pyrimidine strand (Figure 4A). This behavior indicates that the structure formed at low temperature in the presence of magnesium ion has some non-cooperative base stacking and also that the dissociated oligomer has residual structure. Normalized temperature profiles in 0.05 M $MgCl_2$ at different concentrations of d(AG)$_8$ (Figure 6B) show that the temperature of the transition increases directly with the activity of the purine strand. An inset gives the concentration dependence of the apparent T_m. These data provide strong evidence for the formation of a self-associated, intermolecular complex by

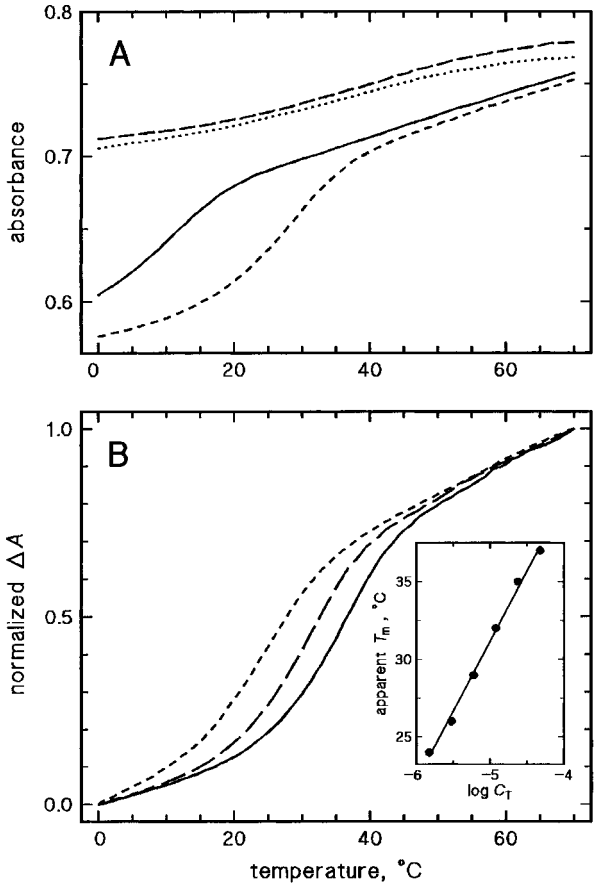

FIGURE 6: UV thermal profiles at 255 nm for purine oligomers at pH 8 in 0.1 M NaCl. (A) d(AG)$_8$ without [—] and with [- - -] additional 0.05 M $MgCl_2$; d(AG)$_8$ without [— —] and with [···] additional 0.05 M $MgCl_2$. (B) Concentration dependence of d(AG)$_8$ with additional 0.05 M $MgCl_2$. Normalized thermal profiles [$\Delta A = (A_{T,°C} - A_{0°C})/(A_{70°C} - A_{0°C})$] at 48 [—], 12 [— —], and 3 [- - -] μM. Inset is the dependence of apparent T_m on log C_T.

the phosphodiester purine strand in the presence of magnesium ion. The absorption maximum for d(AG)$_8$ shifts from 252 nm at 0 °C to 255 nm at 70 °C, again suggesting the guanosine residues as being active participants in the self-complex. The absorption maximum of the d(AG)$_8$ analog remains at 256 nm at all temperatures and ionic conditions investigated. The d(CT)$_8$ oligomer has an overall hyperchromicity of less than 2% at its absorption maximum (268 nm), indicating negligible self-structure in the single-stranded state.

NMR Spectroscopy. Base-pairing interactions in the hybrid duplex and triplex were examined by NMR observation of the hydrogen-bonded imino protons in aqueous solution. Spectra at 30 °C for two d(CT)$_8$:d(AG)$_8$ mixtures are shown in Figure 7A. At 1:1 pyr:pur strand stoichiometry, major resonance envelopes at 12.6 and 13.7 ppm are observed. A tentative assignment for these proton types can be made by comparison to the spectrum of the d(CT)$_8$·d(AG)$_8$ duplex at pH 8.2. Two envelopes were also observed for the parent duplex and were assigned to hydrogen-bonded imino protons of W·C G·C (12.6 ppm) and A·T (13.7 ppm) base pairs (Kan et al., 1991). The hybrid duplex shows some differences from the parent in that the downfield envelope has a distinct shoulder at 13.5 ppm which may be due to stereoisomer effects at the methylphosphonate backbone. Also, a very broad resonance is detected around 12 ppm. It is interesting to note that chemical shifts observed for the

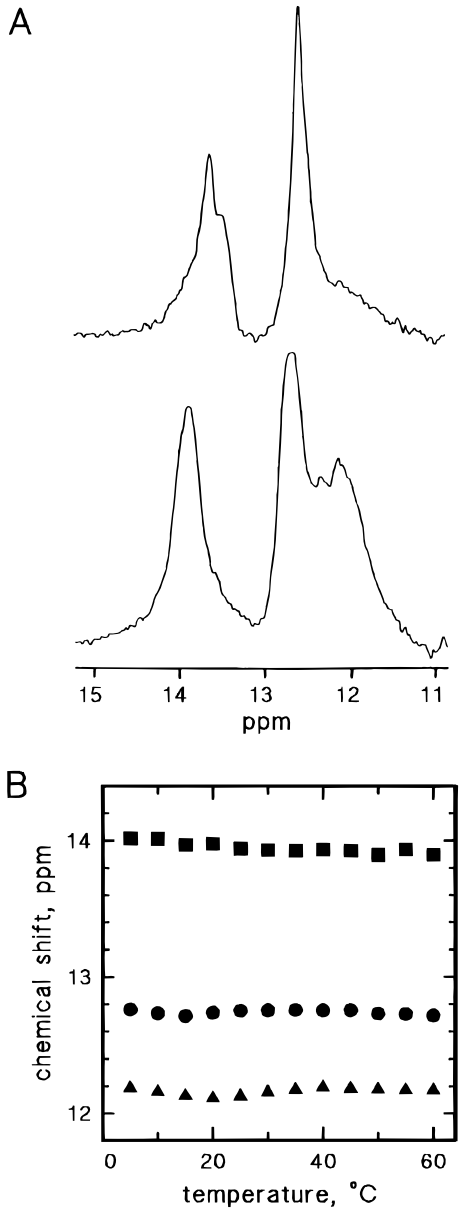

FIGURE 7: Hydrogen-bonded imino proton resonances at 300 MHz for d(CT)$_8$:d(AG)$_8$ mixtures at pH 8 in 0.1 M Na^+. (A) Spectra at 30 °C for [1 mM]:[1mM] (upper) and [1 mM]:[2 mM] (lower) mixtures. (B) Temperature dependence of imino proton resonances observed for the 1:2 mixture. T·A base pairs (W·C) [■]; C·G base pairs (W·C) [●]; third-strand guanosines [▲].

hydrogen-bonded imino protons of the hybrid duplex are very similar to those found for the parent complex, in spite of the differences exhibited by their CD spectra. Several changes occur in this spectral region upon addition of another equivalent of d(AG)$_8$ strand to the 1:1 sample. The original two major resonance envelopes broaden and shift downfield to 12.7 and 13.9 ppm, and a new distinct envelope appears at 12.2 ppm. The adenine bases do not have imino-type protons at these conditions; therefore, the additional high-field resonance envelope is most likely due to hydrogen-bonding of imino protons from guanosine residues in the third strand. This is clear evidence that the additional methylphosphonate purine oligomer is binding to the hybrid duplex through base-pairing interactions. The broad resonance observed in this region for the 1:1 mixture suggests that the hybrid triplex may exist as a small fraction of the hydrogen-bonded species at this mole ratio of complementary oligomers. Temperature dependence of the imino resonances for the hybrid triplex is shown in Figure 7B. The three envelopes are clearly observable up to 60 °C, above which they simultaneously disappear from the spectrum. This temperature is higher than that observed for dissociation of the complex in the optical studies due to the higher concentration of interacting strands in the NMR sample. The thermal behavior of these exchangeable, hydrogen-bonded resonances is consistent with the triplex dissociating directly to single strands, thereby supporting interpretation of the UV thermal profile.

Native Gel Electrophoresis. Duplex or triplex formation with the pyrimidine strand, d(CT)$_8$, by either phosphodiester or methylphosphonate purine oligomers will result in complexes of different size and charge density. These complexes should exhibit differential mobilities during electrophoretic transport through a gel matrix under conditions which support complex formation. Using an oligomeric pyr:pur model system, single-, double-, and triple-stranded species were shown to have relatively decreasing mobilities in a native PAGE experiment (Shea et al., 1990). A hybrid phosphodiester−methylphosphonate duplex or triplex with one-half, one-third, or two-thirds of the backbone charge eliminated should have decreased electrophoretic mobility with respect to the corresponding parent complex composed entirely of negatively-charged phosphodiester oligomers. Therefore, a gel-shift assay should be useful to detect duplex and triplex formation in the model system studied here. However, unlike the optical experiments in which the concentrations of interacting components are fixed, mixtures of species with different electrophoretic mobilities may not remain constant during a PAGE experiment, thereby disrupting the initial, established equilibrium. When considering a native gel-shift assay, the electrophoretic properties of the uncomplexed oligomers themselves are an important factor. Specifically, a single-stranded methylphosphonate oligomer is expected to have the least mobility in a PAGE experiment, whereas a single-stranded phosphodiester oligomer will have the greatest. If a hybrid complex should dissociate at any time during electrophoresis, its single-stranded components will be rapidly separated due to the large difference in their mobilities. Such a process will result in dilution of the effective concentrations of these interacting species. In contrast, this situation will be different for complexes formed between phosphodiester oligomers having approximately equivalent mass and charge. In the case of temporary strand separation during a dissociation event, these single-stranded oligomers will have similar mobilities, thus preserving an effective binding concentration at their location in the gel. Considering these mobility differences between nonionic and charged species, it should be more difficult to detect hybrid phosphodiester−methylphosphonate complexes than the usual charged complexes using a gel-shift assay.

An autoradiograph of a polyacrylamide gel in which oligomers were electrophoresed in 0.1 M NaCl is shown in Figure 8. In order to limit dissociation of complexes and rate of separation of negatively-charged and nonionic single strands, electrophoresis was carried out at low temperature (4 °C) and low field (2.5 V/cm). Bands detected on the gel are due to either 5′-end-labeled d(CT)$_8$ phosphodiester (lanes 1−12) or to 5′-end-labeled d(AG)$_8$ methylphosphonate (lanes 13−17). As expected, single-stranded d(CT)$_8$ has the greatest mobility of all species detected (lanes 1 and 6) and

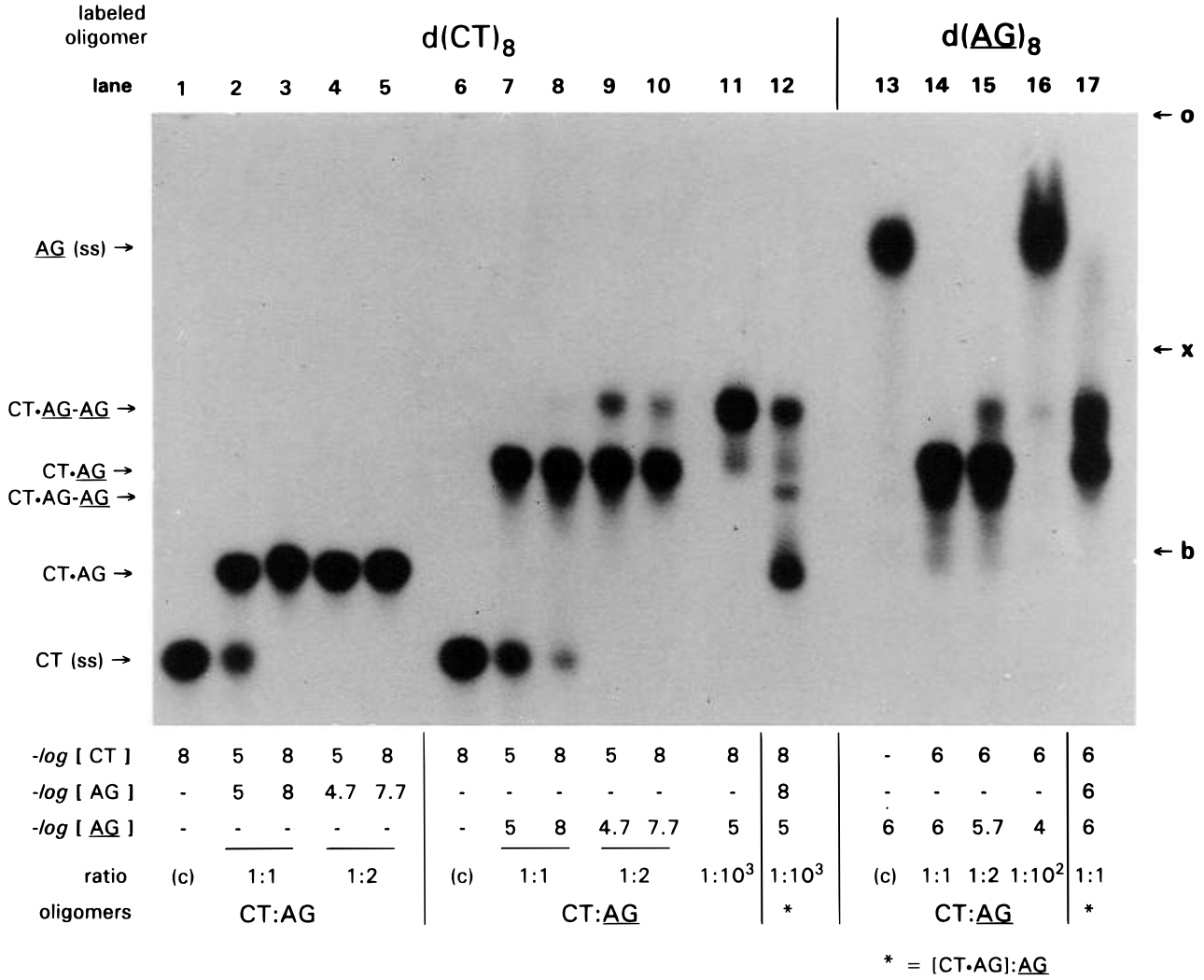

FIGURE 8: Autoradiograph of a native polyacrylamide gel with ^{32}P-end-labeled d(CT)$_8$ (lanes 1−12) or d(AG)$_8$ (lanes 13−17). Concentrations (in negative log units) of d(CT)$_8$, d(AG)$_8$, and d(AG)$_8$ oligomers in the hybridization mixtures are given below each lane along with their molar ratios ("c" denotes control lane having single-stranded, labeled oligomer, only). Positions of various oligomeric species and their complexes are indicated at the left. Positions of the origin (o) and of marker dyes xylene cyanol (x) and bromophenol blue (b) are indicated at the right.

single-stranded d(AG)$_8$ has the least (lane 13). The labeled methylphosphonate oligomer has some electrophoretic mobility as it contains three negative charges at these conditions: one from the single phosphodiester 5′-internucleoside backbone linkage and two from the enzymatically-added 5′-terminal phosphate. All other bands detected between these single-stranded species are inferred to be the result of specific complex formation. Mixtures of d(CT)$_8$:d(AG)$_8$ and d(CT)$_8$:d(AG)$_8$ at various stoichiometries and strand concentrations were examined.

Only one band of lower mobility than the pyrimidine single strand is detected in 1:1 and 1:2 d(CT)$_8$:d(AG)$_8$ mixtures (lanes 2−5) at 10^{-5} and 10^{-8} M strand concentrations. This species can be attributed to the parent W•C duplex. No other shifted band is observed in these mixtures. This result confirms the optical studies by showing that only one specific complex is formed by the phosphodiester pyrimidine and purine strands and that a pyr•pur-pur triplex is not formed at 4 °C in 0.1 M NaCl. However, when the methylphosphonate purine strand is mixed with the phosphodiester pyrimidine oligomer, two different complexes can be readily detected on the gel. Mixtures at 1:1 d(CT)$_8$:d(AG)$_8$ (lanes 7 and 8) show the presence of only one additional band which has decreased mobility compared to the parent duplex. This band is, therefore, assigned to the presence of the hybrid duplex which will have approximately one-half of the negative charge of the parent. Two species of slower mobility are detected in 1:2 d(CT)$_8$:d(AG)$_8$ mixtures (lanes 9 and 10). The more intense band has the same mobility as those detected in 1:1 mixtures and is assigned to the hybrid duplex. A band of even slower mobility is seen as a minor species in the 1:2 mixtures and can be attributed to the presence of the hybrid triplex. By increasing the methylphosphonate oligomer concentration by three orders of magnitude over that of its complement (1:1000 mixture, lane 11) the hybrid d(CT)$_8$•d(AG)$_8$-d(AG)$_8$ triplex is clearly detected as the major complex with d(CT)$_8$. A small amount of residual, uncomplexed 5′-[^{32}P]-d(CT)$_8$ is observed in the 1:1 mixtures in lanes 2, 6, and 7. This phenomenon may be due a small inequivalence in strand stoichiometry and to the preferential binding of unlabeled, unphosphorylated d(CT)$_8$, which is in large excess over the labeled species, to the purine oligomers. Mixtures at 1:1, 1:2 and 1:100 d(CT)$_8$:d(AG)$_8$ using end-labeled methylphosphonate oligomer (lanes 14−16) confirm the presence and the relative mobilities of the hybrid duplex and triplex. In the latter mixture, however,

only a faint triplex band is seen, as most of the labeled oligomer remains with the excess pool of single-stranded d(AG)$_8$.

The three-component d(CT)$_8$·d(AG)$_8$-d(AG)$_8$ triplex was also investigated using native PAGE. As shown in the UV mixing study, addition of d(AG)$_8$ to a 1:1 d(CT)$_8$:d(AG)$_8$ mixture at room temperature resulted in replacement of the phosphodiester purine strand in the parent duplex by its nonionic counterpart. The possibility of such strand exchange was considered during sample preparation for the gel experiment. Using end-labeled pyrimidine strand as a marker, a mixture of [d(CT)$_8$·d(AG)$_8$]:d(AG)$_8$ at 1:1000 molar ratio was electrophoresed in lane 12. The sample was prepared by annealing the parent duplex to 4 °C and then adding the methylphosphonate oligomer on ice. These hybridization conditions were chosen in order to minimize dissociation of the preformed d(CT)$_8$·d(AG)$_8$ duplex. Four species containing labeled d(CT)$_8$ were separated on the gel. The fastest and slowest moving bands are of greatest intensity and have the same mobilities as the parent duplex and 1:2 d(CT)$_8$:d(AG)$_8$ hybrid triplex, respectively. Due to excess methylphosphonate oligomer it is not surprising that the latter complex is present, as dissociation of the parent duplex would result predominantly in its formation. A faint band having the same mobility as the hybrid duplex is also detected. The remaining band has a mobility which is intermediate between both parent and hybrid duplexes. This species is therefore assigned to a triplex having the desired 1:1:1 d(CT)$_8$:d(AG)$_8$:d(AG)$_8$ stoichiometry. Although the relationship of the three strands to each other cannot be confirmed by such an experiment, this triplex is inferred to be one in which the methylphosphonate purine strand is bound as a third strand to an underlying parent duplex. Placing the label on the d(AG)$_8$ oligomer in a 1:1 [d(CT)$_8$·d(AG)$_8$]:d(AG)$_8$ mixture shows two poorly resolved bands, probably due to the formation of hybrid duplex and triplex only (lane 17).

DISCUSSION

The most significant finding of the studies presented here is that the nonionic methylphosphonate purine oligomer, d(AG)$_8$, is able to form a pyr·pur-pur triplex through intermolecular interaction with the negatively-charged phosphodiester pyrimidine oligomer, d(CT)$_8$. Formation of the d(CT)$_8$·d(AG)$_8$ complex is not surprising as duplex formation between methylphosphonate oligomers and complementary phosphodiester sequences is well-established (Bower et al., 1987; Sarin et al., 1988; Lin et al., 1989). This hybrid duplex plays an important role in triplex formation in the model system. The third-strand d(AG)$_8$ oligomer presumably binds, through specific pur-pur base-pairing interactions, to the d(AG)$_8$ strand in the underlying duplex structure. The nonionic purine oligomer is remarkable, in terms of its ability to form interstrand complexes, in that it has very little self-interaction *except when the complementary d(CT)$_8$ strand is present*. The optical data indicate that the conformation of the d(CT)$_8$·d(AG)$_8$ duplex differs from that of the phosphodiester complex. The hybrid duplex readily converts to a triplex through binding of the third-strand d(AG)$_8$ oligomer, as evidenced by the relative stabilities of the two complexes. Consequently, the d(CT)$_8$·d(AG)$_8$-d(AG)$_8$ triplex is formed whenever the nonionic purine strand is in excess of the charged pyrimidine strand. This unique ability of d(AG)$_8$ to interact with itself through a duplex framework apparently results from properties contributed by the methylphosphonate backbone linkage. Reduced negative-charge density in the hybrid complexes does favor their formation in this system as demonstrated by the relative insensitivity of their helix−coil transitions to counterion effects. However, electrostatic factors cannot, by themselves, explain the intermolecular interactions of d(AG)$_8$, especially the inability of this nonionic purine oligomer to self-associate as compared to the negatively-charged parent oligomer, d(AG)$_8$. It is possible that the methylphosphonate linkage modifies the electronic properties of the nonionic backbone so as to configurationally allow particular interactions to occur. In other words, backbone configurations of the d(AG)$_8$ oligomer within the hybrid duplex may facilitate, or more easily accommodate, third-strand binding. Steric interactions or stereoisomer heterogeneity at the phosphonate methyl do not appear to be destabilizing factors in complex formation for this model system. We attempted to determine if the nonionic d(AG)$_8$ oligomer might bind to the parent d(CT)$_8$·d(AG)$_8$ duplex, thereby forming a pyr·pur-pur hybrid triplex. While this species could be detected by native PAGE under carefully controlled conditions, the negatively-charged duplex is probably not a good target for the binding of a purine methylphosphonate oligomer as a third strand only. The hybrid triplex is more stable than the parent duplex at moderate temperatures and ionic conditions. The propensity of the purine phosphodiester oligomer to form a self-structure may also enhance its dissociation from the parent duplex, thereby making the charged pyrimidine strand available to bind to the nonionic complement.

Several base triad geometries may be proposed for the structure of the d(CT)$_8$·d(AG)$_8$-d(AG)$_8$ hybrid triplex. Four schemes under consideration are shown in Figure 9. The envelope observed at 12.2 ppm in the NMR studies is consistent with third-strand guanosine residues pairing via imino protons to the duplex; therefore, triads showing such hydrogen bonds are given in the upper part of each scheme. Triads having third-strand adenosine pairings which are geometrically compatible are shown below. As the sequence utilized in our model system consists of a dinucleotide repeat, the pyr·pur-pur base-pairings may arise from either C·G-G and T·A-A or T·A-G and C·G-A interactions. In addition, regularity of the sequence does not allow for unambiguous assignment of relative orientations for the second and third strands. The first proposed pair of triads (Figure 9A) are based upon C·G-G and U·A-A tertiary interactions found in tRNA (Kim, 1987). Note that these two triads are not strictly isomorphic in that the third-strand guanosine hydrogen bonds at N1 and N2 whereas the third-strand adenosine utilizes N6 and N1. The second and third strands are oriented antiparallel; therefore, such a pairing geometry would result in an unused residue at one end of the third strand and an unbound base pair at the other end of the duplex. Pyr·pur-pur triplexes involving guanosine-rich phosphodiester strands form according to the C·G-G interaction shown here (Beal & Dervan, 1991; Radhakrishnan et al., 1991). NMR studies on such triplexes have found chemical shifts of 13−14 ppm for third-strand guanosine N1H hydrogen-bonded to second-strand guanosine N7 (Radhakrishnan, et al., 1991; Dittrich et al., 1994). The second pair of triad geometries (Figure 9B) are modeled after the parallel G-G base pairing found in G-tetrad structures. NMR observation of such complexes

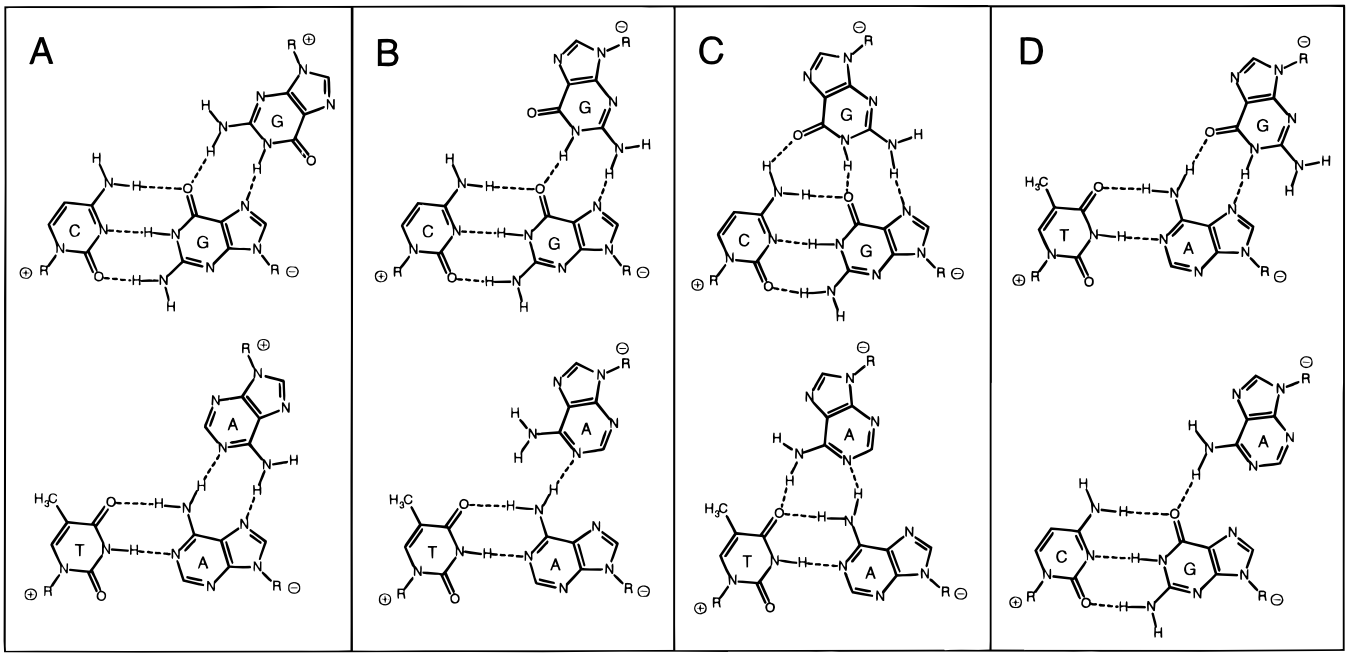

FIGURE 9: Base triad schemes having pur-pur base-pairing interactions considered for the d(CT)$_8$·d(AG)$_8$-d(AG)$_8$ triplex. (A) Triads based on C·G-G and U·A-A tRNA tertiary interactions. (B) Triads based on G-G base-pairing geometry found in G-tetrads. (C) Triads based on proposed intermediate triplex formed during homologous recombination (R-form). (D) Triads based on A-G base-pairing found in A(*syn*)·G-(*anti*) W·C mismatch. In each triad the W·C base pair is oriented along the lower edge and the third-strand residue is oriented at the top right. Hydrogen bonds are indicated by dashed lines and relative backbone orientations (⊕ or ⊖) are indicated at glycosyl linkages to sugars (R).

have found chemical shifts of 11−12 ppm for guanosine N1H hydrogen-bonded to guanosine O6 (Jin et al., 1990; Smith & Feigon, 1992). In order to construct an isomorphous T·A-A triad, only one hydrogen bond can be formed between second- and third-strand adenosines. Assuming all glycosyl torsion angles in the third strand to be *anti*, this pairing configuration would result in parallel pur-pur strand orientation. The third set of triads (Figure 9C) are based upon pairing interactions proposed as an intermediate triplex state (R-form) in homologous recombination mediated by RecA protein (Zhurkin et al., 1994). These geometries are related to the second schemes by an in-plane rotation of the third-strand bases toward the center of the major groove of the W·C dyad. This permits additional hydrogen bonding between groups on the first and third strands. Although the geometries of these patterns appear noncanonical, the C·G-G triad as shown has been observed in a DNA crystal structure (Schultz et al., 1991). The final set of triads (Figure 9D) is patterned after an A(*syn*)·G(*anti*) mismatch base pairing found in certain W·C duplexes (Brown et al., 1986) and has parallel pur-pur strand orientation. Isomorphic T·A-G and C·G-A triads are shown, with the latter having only one hydrogen bond in the pur-pur interaction. This pairing configuration would also result in unpaired bases at opposite ends of the duplex and third strands.

We have carried out various experiments in order to more clearly define the structure of the hybrid triplex. We attempted to discern if there were any NOE observable distances to the third-strand, hydrogen-bonded imino resonance envelope of the hybrid triplex. NMR experiments at several observation frequencies were unable to provide evidence that the protons resonating at 12.2 ppm were in close proximity to any aromatic protons in the structure (L.-S. Kan and T. L. Trapane, unpublished experiments). In case of the pairings shown in Figure 9A or 9D, an NOE between H8 of second-strand guanosine or adenosine residues, respectively, should have been observed. We have also attempted to scramble the sequence in order to determine the relative orientations of the second and third strands. Complementary antiparallel pyr·pur duplexes were verified by mixing curve analyses for two such sequences. Methylphosphonate third strands designed to bind with antiparallel pur-pur orientations had absolutely no interactions with these duplexes. However, triplexes at 1:2 pyr:pur stoichiometry could not be clearly demonstrated for these non-symmetrical sequences (T. L. Trapane and P. O. P. Ts'o, unpublished experiments). These trials indicate that the dinucleotide repeat is important to the formation of a pyr·pur-pur triplex in this model system. In addition, studies involving RNA pyrimidine targets, both with alternating and scrambled sequence, indicate that a parallel pur-pur binding is favored for methylphosphonate purine strands in hybrid triplexes (Reynolds et al., 1994). The base triads in Figure 9A are not favored, due to considerations of strand polarity and the low-field chemical shift observed for antiparallel pyr·pur-pur triplexes formed by phosphodiester strands. Although the chemical shift we observe is close to the range found for G-tetrad structures, we note that modification of all adenosine residues in d(AG)$_8$ to 2-aminopurine in a methylphosphonate oligomer exhibited very poor binding to both d(CT)$_8$·d(AG)$_8$ and d(CT)$_8$·d(AG)$_8$ duplexes (T. L. Trapane, Y. Zhou, and P. O. P. Ts'o, unpublished experiments). The 6-amino group of adenosine, therefore, must also be important to the structure of the hybrid triplex. Considering these three factors, (i) probable parallel pur-pur strand orientation, (ii) chemical shift of the third-strand guanosine N1H approximate to that of G-tetrad, and (iii) importance of the NH6 group of adenosine, we consider the triads shown in Figure 9C to be the most consistent with our understanding of the structure of the hybrid triplex. More structural information

must be obtained before the base-pairing geometries of the hybrid triplex can be unambiguously determined.

The intermolecular interactions of the negatively-charged $d(AG)_8$ oligomer differ greatly from its nonionic analog. Although the expected W·C duplex is readily observed, formation of a $d(CT)_8$·$d(AG)_8$-$d(AG)_8$ triplex could not be clearly demonstrated. The phosphodiester purine oligomer is remarkable in that it readily self-associates, a process which is facilitated by low temperature, high strand activity, and unusually high magnesium ion concentrations. Formation of intramolecular, pyr·pur-pur, H-form triplexes involving $d(CT)_n$·$d(AG)_n$ sequence stabilized by divalent cations has been reported (Bernués et al., 1989; Baran et al., 1991). We chose magnesium as a divalent cation which might stabilize pyr·pur-pur triplex formation by phosphodiester strands as many studies indicate a requirement for this cation (Cooney et al., 1988; Kohwi & Kohwi-Shigematsu, 1988; Baran et al., 1991; Beal & Dervan, 1991; Pilch et al., 1991). The amount of Mg^{2+} needed to stabilize the self-complex at 20 °C in our model system is well above that required as counterion for the negative backbone charge. Therefore, the divalent cation may be mediating the self-association process through interactions in addition to those at phosphate groups. Certain nucleic acid sequences with high purine content are known to coordinate cations at the purine bases. In particular, sequences occurring at recombination and telomere sites have been shown to form a tetra-stranded complex through the binding of a monovalent cation between stacked G-tetrads (Jin et al., 1990; Kang et al., 1992; Smith & Feigon, 1992). Also, divalent cations have a high affinity for binding to purine bases, particularly at N7 (Saenger, 1984). The self-association phenomenon observed for the phosphodiester purine oligomer in this model system may result from similar interactions in which paired, stacked base moieties can coordinate the cation. The phosphodiester backbone is necessary for self-complex formation, as modification to the nonionic linkage eliminates this interaction in an otherwise identical oligomer. Guanosine residues in the sequence also appear to be involved, as the optical data reflect participation of these moieties in formation of the self-complex. It is not possible to determine the number of strands interacting to form this self-complex using the methods employed here. However, it should be noted that self-association at a variety of environmental conditions has been previously reported for purine polymers and oligomers having the same or similar sequence (Antao et al., 1988; Feigon et al., 1990; Lee, 1990; Rippe et al., 1992; Dolinnaya & Fresco, 1992). In these studies, purine self-association could occur at a variety of conditions, with tetra-, double-, and single-stranded conformations proposed. It is also noteworthy that the self-complex observed for $d(AG)_4$ (50 mM NaCl, 5 mM $MgCl_2$, pH 7, 1 °C) has a strong G-G hydrogen-bonded imino resonance envelope at 12 ppm (Feigon et al., 1990), similar to that observed for the hybrid triplex. The strong self-association tendency of $d(AG)_8$ to form a higher-order complex at various environmental conditions appears to be an interesting model which may be pertinent to the understanding of pur-pur interactions involving naturally-occurring nucleic acids. The formation of pyr·pur-pur triplexes by phosphodiester strands which require guanosine residues and the presence of specific cations has been reported by others (Cooney et al., 1988; Bernués et al., 1990; Lyamichev et al., 1991; Beal & Dervan, 1991; Pilch et al., 1991; Orson et al., 1991; Malkov et al., 1993). The tendency of such purine-rich strands to self-interact should be kept in mind when proposing hydrogen-bonding schemes and base specificities for these types of triplexes.

Formation of the $d(CT)_8$·$d(\underline{AG})_8$-$d(\underline{AG})_8$ triplex is significant in regard to the understanding of nucleic acid structures and their possible application to biological problems. From a physical standpoint, the model system developed here may afford insights into the conformation of pur-pur interactions at mixed purine sequence. In addition, the ability of methylphosphonate purine oligomers to form triplexes of high stability at single-stranded pyrimidine target sites in DNA or RNA may enable inhibition of biochemical processes occurring at these sites *in vivo* (Reynolds et al., 1994).

ACKNOWLEDGMENT

We thank Scott Morrow of the DNA Synthesis Facility, Department of Biochemistry, The Johns Hopkins University, for preparing the phosphodiester oligomers and Dr. David Shortle of the Department of Biological Chemistry, The Johns Hopkins University, for providing the CD spectropolarimeter. We are grateful to Dr. Mary Claire Shiber for advice regarding the gel experiment and to Drs. Paul Miller and Dan Callahan for helpful discussions.

REFERENCES

Albergo, D. D., Marky, L. A., Breslauer, K. J., & Turner, D. H. (1981) *Biochemistry 20*, 1409−1413.

Antao, V. P., Gray, D. M., & Ratliff, R. L. (1988) *Nucleic Acids Res. 16*, 719−738.

Baran, N., Lapidot, A., & Manor, H. (1991) *Proc. Natl. Acad. Sci. U.S.A. 88*, 507−511.

Beal, P. A., & Dervan, P. B. (1991) *Science 251*, 1360−1363.

Bernués, J., Beltrán, R., Casasnovas, J. M., & Azorín, F. (1990) *Nucleic Acids Res. 18*, 4067−4073.

Bower, M., Summers, M. F., Powell, C., Shinozuka, K., Regan, J. B., Zon, G., & Wilson, W. D. (1987) *Nucleic Acids Res. 15*, 4915−4930.

Breslauer, K. J., Frank, R., Blöcker, H., & Marky, L. A. (1986) *Proc. Natl. Acad. Sci. U.S.A. 83*, 3746−3750.

Broitman, S. L., Im, D. D., & Fresco, J. R. (1987) *Proc. Natl. Acad. Sci. U.S.A. 84*, 5120−5124.

Brown, T., Hunter, W. N., Kneale, G., & Kennard, O. (1986) *Proc. Natl. Acad. Sci. U.S.A. 83*, 2402−2406.

Bush, C. A. (1974) in *Basic Principles in Nucleic Acid Chemistry* (Ts'o, P. O. P., Ed.) Vol. 2, pp 91−169, Academic Press, New York.

Callahan, D. E., Trapane, T. L., Miller, P. S., Ts'o, P. O. P., & Kan, L.-S. (1991) *Biochemistry 30*, 1650−1655.

Chastain, M., & Tinoco, I. (1992) *Nucleic Acids Res. 20*, 315−318.

Cooney, M., Czernuszewicz, G., Postel, E. H., Flint, S. J., & Hogan, M. E. (1988) *Science 241*, 456−459.

Dittrich, K., Gu, J., Tinder, R., Hogan, M., & Gao, X. (1994) *Biochemistry 33*, 4111−4120.

Dolinnaya, N. G., & Fresco, J. R. (1992) *Proc. Natl. Acad. Sci. U.S.A. 89*, 9242−9246.

Feigon, J., Gilbert, D., Rajagopal, P., Wang, E., van der Marel, G. A., & van Boom, J. H. (1990) in *Structure and Methods* (Sarma, R. H., & Sarma, M. H., Eds.) Vol. 3, pp 207−224, Adenine Press, Schenectady, NY.

Felsenfeld, G., Davies, D. R., & Rich, A. (1957) *J. Am. Chem. Soc. 79*, 2023−2024.

François, J.-C., Saison-Behmoaras, T., Thuong, N. T., & Hélène, C. (1989) *Biochemistry 28*, 9617−9619.

Gray, D. M., Ratliff, R. L., Antao, V. P., & Gray, C. W. (1987) in *Structure and Expression* (Sarma, R. H., & Sarma, M. H., Eds.) Vol. 2, pp 147−166, Adenine Press, Schenectady, NY.

Harned, H. S., & Owen, B. B. (1967) in *The Physical Chemistry of Electrolyte Solutions*, 3rd ed., pp 585−632, Rheinhold, New York.
Hore, P. J. (1983) *J. Magn. Reson. 55*, 283−300.
Howard, F. B., Miles, H. T., & Ross, P. D. (1995) *Biochemistry 34*, 7135−7144.
Jin, R., Breslauer, K. J., Jones, R. A., & Gaffney, B. L. (1990) *Science 250*, 543−546.
Job, P. (1928) *Ann. Chim. (Paris) 9*, 113−134.
Johnson, W. C. (1985) *Methods Biochem. Anal. 31*, 61−163.
Kan, L.-S., Callahan, D. E., Trapane, T. L., Miller, P. S., Ts'o, P. O. P., & Huang, D. H. (1991) *J. Biomol. Struct. Dyn. 8*, 911−933.
Kang, C., Zhang, X., Ratliff, R., Moyzis, R., & Rich, A. (1992) *Nature (London) 356*, 126−131.
Kibler-Herzog, L., Kell, B., Zon, G., Shinozuka, K. Mizan, S., & Wilson, W. D. (1990) *Nucleic Acids Res. 18*, 3545−3555.
Kim, S.-H. (1987) *Adv. Enzymol. 46*, 279−315.
Kohwi, Y., & Kohwi-Shigematsu, T. (1988) *Proc. Natl. Acad. Sci. U.S.A. 85*, 3781−3785.
Lee, J. S. (1990) *Nucleic Acids Res. 18*, 6057−6060.
Lee, J. S., Johnson, D. A., & Morgan, A. R. (1979) *Nucleic Acids Res. 6*, 3073−3091.
Lee, J. S., Evans, D. H., & Morgan, A. R. (1980) *Nucleic Acids Res. 18*, 4305−4320.
Lesnikowski, Z. J., Jaworska, M., & Stec, W. J. (1990) *Nucleic Acids Res. 18*, 2109−2115.
Lin, S.-B., Blake, K. R., Miller, P. S., & Ts'o, P. O. P. (1989) *Biochemistry 28*, 1054−1061.
Lipsett, M. N. (1963) *Biochem. Biophys. Res. Commun. 11*, 224−228.
Lipsett, M. N. (1964) *J. Biol. Chem. 239*, 1256−1260.
Lyamichev, V. I., Voloshin, O. N., Frank-Kamenetskii, M. D., & Soyfer, V. N. (1991) *Nucleic Acids Res. 19*, 1633−1638.
Maher, L. J., Wold, B., & Dervan, P. B. (1989) *Science 245*, 725−730.
Malkov, V. A., Voloshin, O. N., Soyfer, V. N., & Frank-Kamenetskii, M. D. (1993) *Nucleic Acids Res. 21*, 585−591.
Marck, C., & Thiele, D. (1978) *Nucleic Acids Res. 5*, 1017−1028.
Miller, J. H., & Sobell, H. M. (1966) *Proc. Natl. Acad. Sci. U.S.A. 55*, 1201−1205.
Miller, P. S., Cushman, C. D., & Levis, J. T. (1991) in *Oligonucleotides and Analogues: A Practical Approach* (Ekstein, F., Ed.) pp 137−154, Oxford University Press, Oxford, U.K.
Miller, P. S., Dreon, N., Pulford, S. M., & McParland, K. B. (1980) *J. Biol. Chem. 255*, 9659−9665.
Miller, P. S., McParland, K. B., Jayaraman, K., & Ts'o, P. O. P. (1981) *Biochemistry 20*, 1874−1880.
Morgan, A. R., & Wells, R. D. (1968) *J. Mol. Biol. 37* 63−80.
Moser, H. E., & Dervan, P. B. (1987) *Science 238*, 645−650.
Orson, F. M., Thomas, D. W., McShan, W. M., Kessler, D. J., & Hogan, M. E. (1991) *Nucleic Acids Res. 19*, 3435−3441.
Pilch, D. S., Brousseau, R., & Shafer, R. H. (1990) *Nucleic Acids Res. 18*, 5743−5750.
Pilch, D. S., Levenson, C., & Shafer, R. H. (1991) *Biochemistry 30*, 6081−6087.
Plum, G. E., Park, Y.-W., Singleton, S. F., Dervan, P. B., & Breslauer, K. J. (1990) *Proc. Natl. Acad. Sci. U.S.A. 87*, 9436−9440.
Radhakrishnan, I., de los Santos, C., & Patel, D. J. (1991) *J. Mol. Biol. 221*, 1403−1418.
Rajagopal, P., & Feigon, J. (1989) *Biochemistry 28*, 7859−7870.
Record, M. T., Anderson, C. F., & Lohman, T. M. (1978) *Q. Rev. Biophys. 2*, 103−178.
Reynolds, M. A., Arnold, L. J., Almazan, M. T., Beck, T. A., Hogrefe, R. I., Metzler, M. D., Stoughton, S. R., Tseng, B. Y., Trapane, T. L., Ts'o, P. O. P., & Woolf, T. M. (1994) *Proc. Natl. Acad. Sci. U.S.A. 91*, 12433−12437.
Rippe, K., Fritsch, V., Westhof, E., & Jovin, T. M. (1992) *EMBO J. 11*, 3777−3786.
Saenger, W. (1984) in *Principles of Nucleic Acid Structure*, pp 201−219, Springer-Verlag, New York.
Sarin, P. S., Agrawal, S., Civeira, M. P., Goodchild, J., Ikeuchi, T., & Zamecnik, P. C. (1988) *Proc. Natl. Acad. Sci. U.S.A. 85*, 7448−7451.
Schultz, S. C., Shields, G. C., & Steitz, T. A. (1991) *Science 253*, 1001−1007.
Shea, R. G., Ng, P., & Bischofberger, N. (1990) *Nucleic Acids Res. 18*, 4859−4866.
Shoji, Y., Akhtar, S., Periasamy, A., Herman, B., & Juliano, R. L. (1991) *Nucleic Acids Res. 19*, 5543−5550.
Smith, F., & Feigon, J. (1992) *Nature (London) 356*, 164−168.
Thaden, J., & Miller, P. S. (1993) *Bioconjugate Chem. 4*, 386−394.
Trapane, T. L. (1993) Duplex and Triplex Formation by Oligonucleoside Phosphodiesters and Methylphosphonates, Ph.D. Dissertation, The Johns Hopkins University, Baltimore, MD.
Wells, R. D., Collier, D. A., Hanvey, J. C., Shimizu, M., & Wohlrab, F. (1988) *FASEB J. 2*, 2939−2949.
Zhurkin, V. B., Raghunathan, G., Ulyanov, N. B., Camerini-Otero, R. D., & Jernigan, R. L. (1994) *J. Mol. Biol. 239*, 181−200.

BI960070B